EurJIC
European Journal of Inorganic Chemistry

Chemistry Europe
European Chemical Societies Publishing

Accepted Article

Title: Ligand Effects in Calcium Catalyzed Ketone Hydroboration

Authors: Steffen Brand, Andrea Causero, Holger Elsen, Jürgen Pahl, Jens Langer, and Sjoerd Harder

To be cited as: *Eur. J. Inorg. Chem.* 10.1002/ejic.202000264

Link to VoR: https://doi.org/10.1002/ejic.202000264

WILEY-VCH

10.1002/ejic.202000264

Ligand Effects in Calcium Catalyzed Ketone Hydroboration

Steffen Brand, Andrea Causero, Holger Elsen, Jürgen Pahl, Jens Langer, and Sjoerd Harder*

Inorganic and Organometallic Chemistry, University Erlangen-Nürnberg, Egerlandstrasse 1, 91058 Erlangen, Germany

Prof. Dr. S. Harder, S. Brand, Dr. A. Causero, H. Elsen, Dr. J. Pahl, Dr. J. Langer
E-mail corresponding author: sjoerd.harder@fau.de
Homepage: www.harder-research.com

Keywords: Calcium – Hydroboration – Cationic complexes – Catalysis – Amidinate

Key Topic: Calcium Catalysis

Table of Contents A series of calcium amidinate complexes with various anionic ligands or counter ions were shown to catalyze ketone hydroboration. The influence of ligand variation is discussed. Catalysts with inactive ligands (I^- or $B(C_6F_5)_4^-$) follow a Lewis acid mechanism while those with reactive ligands (H^- or $(Me_3Si)_2N^-$) follow a hydride or borate mechanism.

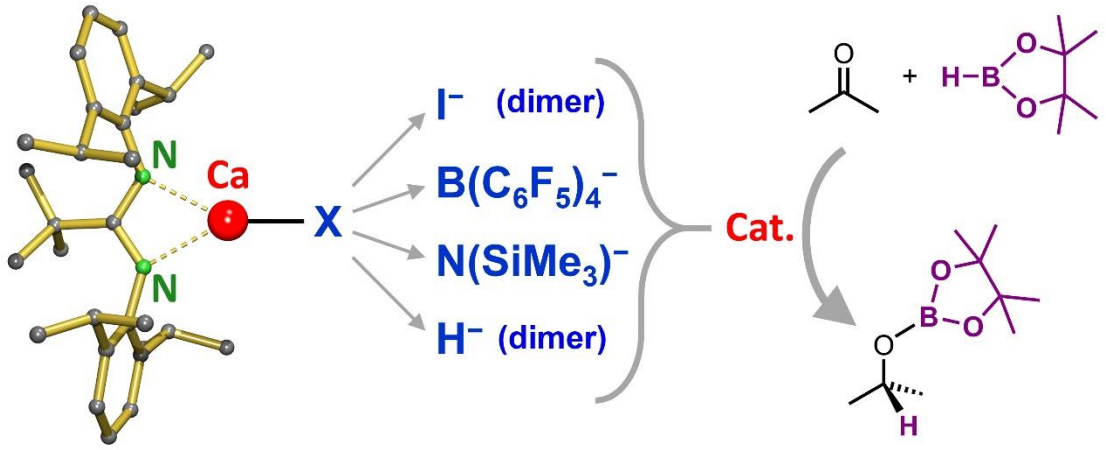

Abstract The first "naked" (Lewis base-free) cationic Ca amidinate complex $[^{tBu}Am^{DIPP}Ca(C_6H_6)]^+[B(C_6F_5)_4]^-$ could be prepared in 62% yield (^{tBu}AmDIPP = *t*BuC(N-DIPP)$_2$; DIPP = 2,6-diisopropylphenyl) by reaction of $[^{tBu}Am^{DIPP}CaH]_2$ with $[Ph_3C]^+[B(C_6F_5)_4]^-$ in chlorobenzene. The ether-free complex $^{tBu}Am^{DIPP}CaN(SiMe_3)_2$ was obtained by removal of diethylether from its ether adduct. Crystal structures show that the amidinate ligand in both complexes is *N,Aryl*-chelating. In this coordination mode the bulk of the amidinate ligand is comparable to that of a DIPP-substituted ß-diketiminate ligand. Isomers with *N,N*-coordinating amidinate ligands are circa 15 kcal/mol higher in energy and this coordination mode is only present in case additional ether ligands compensate for energy loss or in case of space limitation at the metal, e.g. in homoleptic $(^{tBu}Am^{DIPP})_2Ca$. A series of four Ca amidinate complexes, $^{tBu}Am^{DIPP}CaX$, were tested in the catalytic hydroboration of ketones and aldehydes by pinacolborane (HBpin). Catalytic activities increase for $X^- = I^- < B(C_6F_5)_4^- < (Me_3Si)_2N^- \approx H^-$. For catalysts with unreactive anions, like I^- or $B(C_6F_5)_4^-$, catalyst performance increases with the Lewis acidity of the metal and a mechanism is proposed in which HBpin and ketone coordinate to the Ca^{2+} ion which is followed by direct hydroboration. The more active catalysts with $X^- = (Me_3Si)_2N^-$ or H^- likely operate through a mechanism which involves intermediate metal hydride (or borate) complexes.

10.1002/ejic.202000264

Introduction

Over the last decades, research on alkaline earth metal based homogeneous catalysis gained momentum and conquered fields, which were long thought to be the exclusive domain of transition metal catalysis.[1-4] Although often still not on par with their classical transition metal based counterparts, alkaline earth metals make up for lower catalytic activity of their complexes by price, availability and non-toxicity, at least in case of magnesium and calcium. Calcium catalyzed reactions include *inter alia* polymerizations,[5] alkene hydrogenations,[6] alkene and imine hydrosilylation,[7] intramolecular alkene hydroamination,[8] alkene and alkyne hydrophosphination,[9] hydroboration[10] or Mannich-type reactions.[11]

Notwithstanding those successful applications, the conceptual foundation to predict whether a calcium catalyst is highly active for a certain reaction is so far unknown. This is due to the fact that the limited number of reports in calcium catalysis often describe results with drastically different catalysts. Nevertheless, possible factors to influence the reactivity of a catalyst in a given environment are in principle well known and include, but are not limited to, steric demand, charge, donor capacity and donor atom type of spectator ligands, their number and the resulting coordination number of the metal ion, the nuclearity of the resulting complexes and the counter ions present. In general, catalysts of type LCaR consist of a passive spectator L in combination with a reactive group R. The catalytic reaction is based on a combination of substrate activation by the Lewis-acidic Ca^{2+} center and the high nucleophilicity or basicity of R. In some cases, also catalysts that only rely on Lewis acid activation have been reported.[11,12] *E.g.* the Sen group introduced the amidinate calcium iodide catalyst **I** in the hydroboration of ketones and aldehydes.[12] It is unlikely that the highly stable iodide ligand actively takes part in catalysis. In an effort to address the importance of this second anionic ligand, we chose to study the hydroboration of ketones (and aldehydes) as a function of the ligands. We present here a series of catalysts with the bulky amidinate spectator ligand $^{t\mathrm{Bu}}\mathrm{Am}^{\mathrm{DIPP}}$ ($^{t\mathrm{Bu}}\mathrm{Am}^{\mathrm{DIPP}}$ = *t*BuC(N-DIPP)$_2$; DIPP = 2,6-di*iso*propylphenyl) that allowed for the synthesis and isolation of complexes $^{t\mathrm{Bu}}\mathrm{Am}^{\mathrm{DIPP}}$CaX with X^- = I^- (**1**), $[B(C_6F_5)_4]^-$ (**2**), $(Me_3Si)_2N^-$ (**3**) or H^- (**4**); see Scheme 1. The performance of these catalysts will be directly compared with results reported earlier by Sen and coworkers for PhC(N*i*Pr)$_2$CaI(THF)$_3$ (**I**, $^{\mathrm{Ph}}\mathrm{Am}^{i\mathrm{Pr}}$CaI(THF)$_3$).[12]

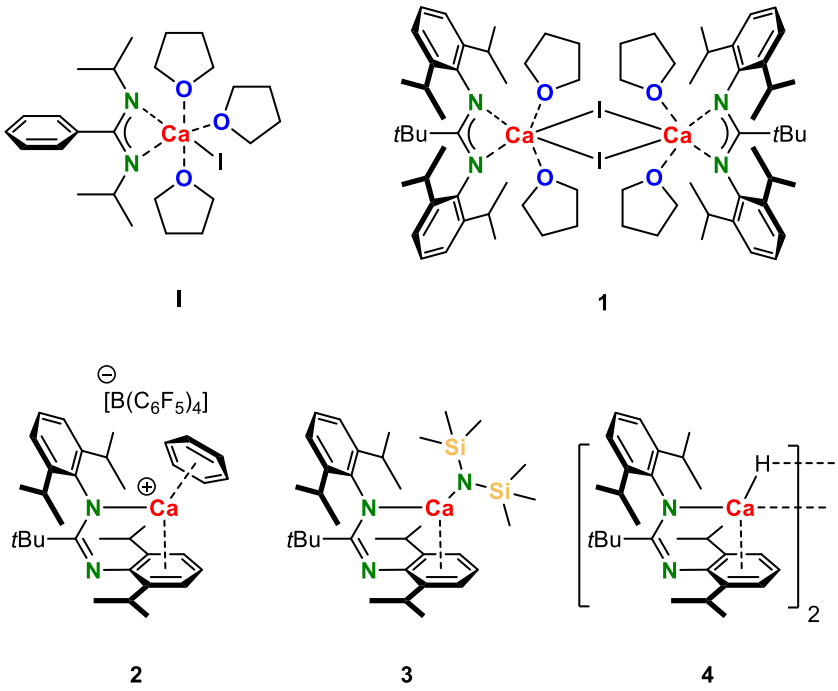

Scheme 1. Previously used calcium based catalyst for the hydroboration of ketones (**I**) and calcium catalysts used in this investigation (**1-4**).

While synthetic strategies for [$^{t\mathrm{Bu}}\mathrm{Am}^{\mathrm{DIPP}}$CaI(thf)$_2$]$_2$ (**1**),[13] $^{t\mathrm{Bu}}\mathrm{Am}^{\mathrm{DIPP}}$CaN(SiMe$_3$)$_2$(Et$_2$O)[14] and [$^{t\mathrm{Bu}}\mathrm{Am}^{\mathrm{DIPP}}$CaH]$_2$ (**4**),[14] are known, synthetic routes had to be developed for [$^{t\mathrm{Bu}}\mathrm{Am}^{\mathrm{DIPP}}$Ca(C$_6H_6$)]$^+$[B(C$_6F_5$)$_4$]$^-$ (**2**) and ether-free $^{t\mathrm{Bu}}\mathrm{Am}^{\mathrm{DIPP}}$CaN(SiMe$_3$)$_2$ (**3**) used in the current investigations.

Results and Discussion

Ligand choice and precatalyst synthesis

Our spectator ligand of choice for the current investigation was $^{tBu}Am^{DIPP}$. This chelating ligand was first reported by Westerhausen and coworkers[15] and previously used in our group for the stabilization of highly reactive calcium hydride complexes,[14] and for Ca derivatives featuring stilbene dianions[13] or novel anionic *N*-heterocyclic olefins.[16] This ligand choice might seem counterintuitive, since $^{tBu}Am^{DIPP}$ has a higher steric demand and lower basicity of its nitrogen atoms when compared to $^{Ph}Am^{iPr}$, used by *Sen* and co-workers[12,17] (buried volume V_B = 34.0% in $[^{tBu}Am^{DIPP}CaI(THF)_2]_2$ (**1**) vs. V_B = 28.1% in $^{Ph}Am^{iPr}CaI(THF)_3$), thus resulting in a less accessible and more electron deficient calcium center. However, its superior adaptability to the changing needs of a bound calcium ion, which is related to a facile interconversion of its *N,N*- and *N,Aryl*-coordination mode,[15,18] makes this ligand almost a requirement, when it comes to the synthesis of one of our envisioned precatalysts, namely $[^{tBu}Am^{DIPP}Ca(C_6H_6)]^+[B(C_6F_5)_4]^-$ (**2**). Related cationic calcium compounds were so far only accessible by the use of the sterically demanding ß-diketiminate ligand $^{Me}BDI^{DIPP}$ ($^{Me}BDI^{DIPP}$ = DIPP-NC(Me)C(H)C(Me)N-DIPP), which has a buried volume of 49.4% in $[^{Me}BDI^{DIPP}Ca(C_6H_6)]^+[B(C_6F_5)_4]^-$ or even 64.1% in $[^{Me}BDI^{DIPP}Ca(C_6H_6)]^+[Al\{OC(CF_3)_3\}_4]^-$.[19,20] Such values seem out of reach for the amidinate $^{tBu}Am^{DIPP}$, which shows V_B's of 34.0% - 40.1% in *N,N*-coordination mode in published calcium complexes, depending on the coordination number (see Table S1, ESI). For the previously unpublished structure of $(^{tBu}Am^{DIPP})_2Ca$ (see Figure 1), the so far highest value of V_B = 42.4% is found for one of the ligands, but the steric shielding provided by $^{tBu}Am^{DIPP}$ in this compound is still significantly lower than for $^{Me}BDI^{DIPP}$ in the above mentioned complexes. This changes drastically, when the ligand adopts a *N,Aryl*-coordination mode. In this conformation, the buried volume of the ligand ranges from 54.7% in $[^{tBu}Am^{DIPP}Ca(NBO\text{-}H)]_2$[16] (NBO-H = deprotonated 1,3-dimethyl-2-methylene-2,3-dihydro-1*H*-imidazole) to 57.6% in $[^{tBu}Am^{DIPP}Ca]_2(SD)$[13] (SD = stilbene dianion), making $^{tBu}Am^{DIPP}$ competitive to $^{Me}BDI^{DIPP}$ when it comes to steric demand (see Table S2, ESI).

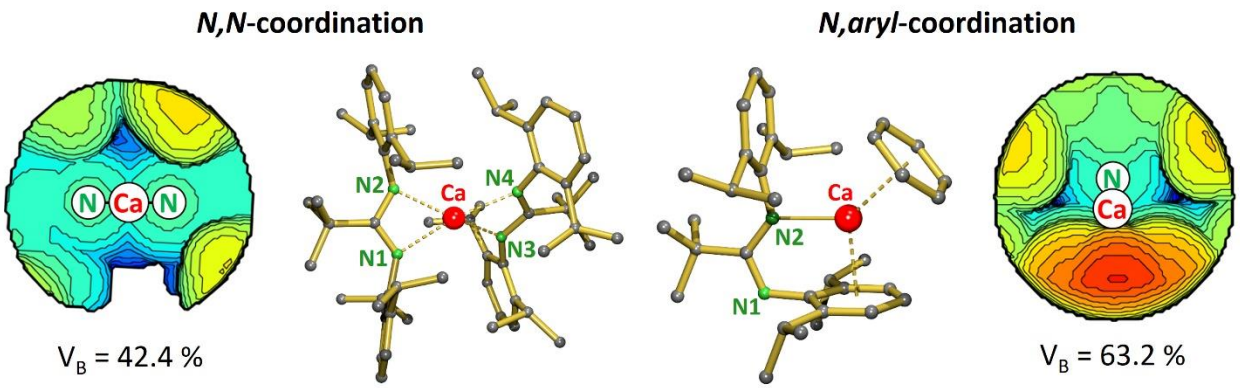

Figure 1. Molecular structures of $[(^{tBu}Am^{DIPP})_2Ca]\cdot$1,4-dioxane (middle left; Hydrogen atoms and co-crystallized 1,4-dioxane have been omitted) and of $[^{tBu}Am^{DIPP}Ca(C_6H_6)]^+[B(C_6F_5)_4]^-$ (middle right; Hydrogen atoms and $[B(C_6F_5)_4]^-$ have been omitted) as well as steric maps for the buried volume in these complexes (in case of $[(^{tBu}Am^{DIPP})_2Ca]$ the bulkier of two ligands was chosen).

With this knowledge at hand, the synthesis of $[^{tBu}Am^{DIPP}Ca(C_6H_6)]^+[B(C_6F_5)_4]^-$ (**2**) was attempted in analogy to the published strategy for $[^{Me}BDI^{DIPP}Ca(C_6H_6)]^+[B(C_6F_5)_4]^-$ (see Scheme 2, left side).[20,21] The required salt $[^{tBu}Am^{DIPP}H_2]^+[B(C_6F_5)_4]^-$ (for XRD data see ESI) was synthesized in 94% yield by treating $^{tBu}Am^{DIPP}H$ with $[HOEt_2]^+[B(C_6F_5)_4]^-$ in chlorobenzene. Unfortunately, addition of solvent-free Ca(*p*-*t*Bu-benzyl)$_2$ to $[^{tBu}Am^{DIPP}H_2]^+[B(C_6F_5)_4]^-$ in chlorobenzene did not lead to a selective reaction, thus precluding the isolation of $[^{tBu}Am^{DIPP}Ca]^+[B(C_6F_5)_4]^-$. Therefore we followed a strategy similar to the one successful for complexes of the type $[^{Me}BDI^{DIPP}Mg(arene)]^+[B(C_6F_5)_4]^-$ (see Scheme 2, right side).[20,22] Addition of $[Ph_3C]^+[B(C_6F_5)_4]^-$ to a suspension of the literature known, donor-free complex $[^{tBu}Am^{DIPP}CaH]_2$[14] in chlorobenzene led overnight to a slow color change from orange-red to brown. After removal of chlorobenzene, a brown foam was obtained which formed a biphasic system upon addition of benzene. The lower phase was washed with benzene until colorless crystals in a sticky brown residue grew. These crystals were suitable for X-ray analysis, but further purification was necessary. The crude product could be crystallized by thermal diffusion in a hexane:benzene (2:1) mixture in good yield (62%) (see Figure S11, ESI).

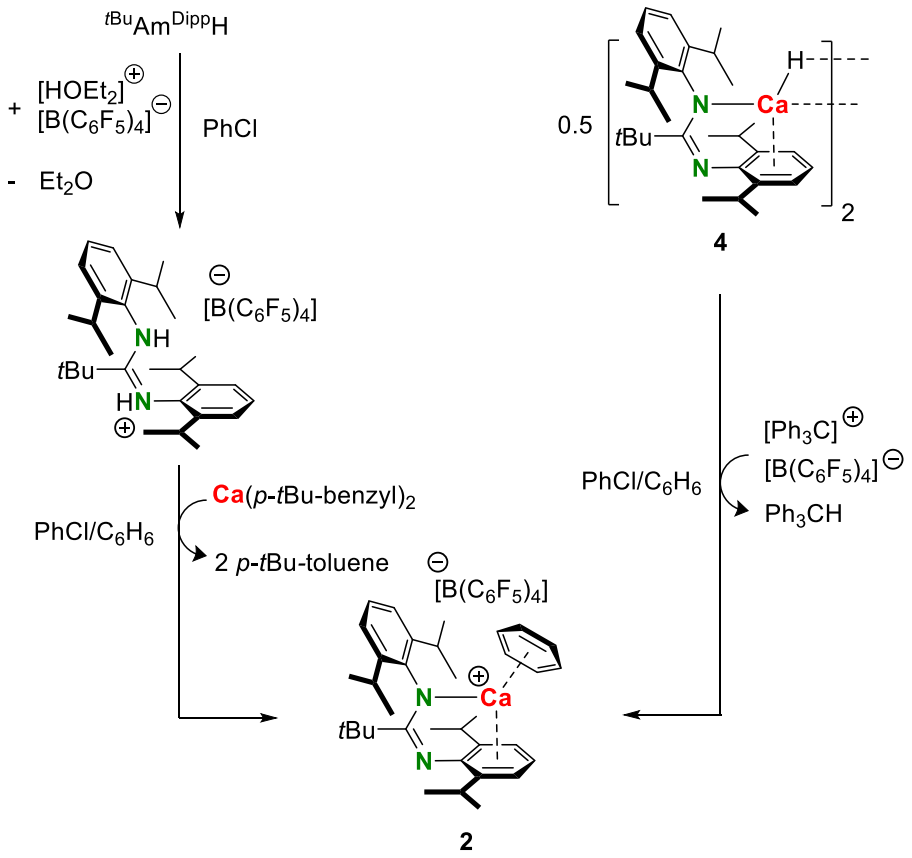

Scheme 2. Explored synthetic routes for $[^{tBu}Am^{DIPP}Ca(C_6H_6)]^+[B(C_6F_5)_4]^-$ (**2**).

XRD structure determination (see Figure 1, Table 1) revealed the retention of the (*N,Aryl*)-coordination mode of the starting material $[^{tBu}Am^{DIPP}CaH]_2$ in $[^{tBu}Am^{DIPP}Ca(C_6H_6)]^+[B(C_6F_5)_4]^-$ (**2**), as well as complete separation of cation and anion. This contrasts with the structure of the ß-diketiminate complex $[^{Me}BDI^{DIPP}Ca(C_6H_6)]^+[B(C_6F_5)_4]^-$ in which a Ca···F contact to the anion persisted. Similar cation-anion separation was earlier observed when *Krossing*'s even weaker coordinating anion $[Al\{OC(CF_3)_3\}_4]$ was employed.[19] In related magnesium complexes, containing the $[B(C_6F_5)_4]^-$ anion, it was necessary to further increase the steric bulk of the BDI ligand by an exchange of Me groups for *t*Bu groups in the ligand backbone, to break the Mg···F interaction.[23]

These findings indicate that the $^{tBu}Am^{DIPP}$ ligand in *N,Aryl*-coordination mode is at least as bulky as the $^{Me}BDI^{DIPP}$ ligand with *N,N*-coordination. This assumption is supported by almost identical values for the volume buried by those ligands in the three-coordinate cations of $[^{tBu}Am^{DIPP}Ca(C_6H_6)]^+[B(C_6F_5)_4]^-$ (**2:** 63.2%) and $[^{Me}BDI^{DIPP}Ca(C_6H_6)]^+[Al\{OC(CF_3)_3\}_4]^-$ (64.1%).

The complete separation of cation and anion in **2** clearly leads to a much higher metal Lewis acidity and consequently shorter bonds to both, N2 and the aryl ring are observed, when compared to contact ion pair $[^{tBu}Am^{DIPP}Ca]_2$(SD). Expectedly, the effect is stronger for the negatively charged nitrogen (**2**: Ca-N2 2.2814(14) Å; $[^{tBu}Am^{DIPP}Ca]_2$(SD): Ca-N2 2.3841(11) Å) than for the η^6-coordinated aryl ring (Ca-$C_{av.}$ 2.8018 Å vs. Ca-$C_{av.}$ 2.839 Å) (see Table 1).

Despite the very strong metal-ligand interaction in **2**, exchange between coordinated and non-coordinated DIPP substituents is not prevented. While at ambient temperature, two distinct sets of ^{1}H NMR signals for the different DIPP moieties are observed (four doublets and two heptets for the *i*Pr substituents), those signals show coalescence upon heating. The activation energy for fast exchange between the two different sides of the amidinate ligand has been estimated from the coalescence temperature of 337 K as $\Delta G^{\ddagger}$ = 16.1 kcal/mol. This value is in the same range as observed for $[^{tBu}Am^{DIPP}CaH]_2$ (**4**, $\Delta G^{\ddagger}$ = 16.8 kcal/mol).[14]

Dissolving complex **2** in bromobenzene-d_5, led to loss of the coordinated benzene ligand and likely coordination of bromobenzene. This is evident from the benzene chemical shift of 7.21 ppm, which is the value of free benzene in this solvent.

10.1002/ejic.202000264

Table 1. Structural comparison of ligand bonding in calcium complexes featuring $^{t\text{Bu}}\text{Am}^{\text{DIPP}}$ (L) in *N,Aryl* coordination mode.

Bond	Bond Lengths [Å]			
	[LCa(C_6H_6)][$B(C_6F_5)_4$] (**2**)	[LCa]$_2$(SD)] [a,b]	[LCaN($SiMe_3$)$_2$] (**3**)	[LCa-(NHO-H)]$_2$ [a,c]
Ca1-N2	2.2814(14)	2.3841(11)	2.3889(19)	2.430(3)
Ca1-C6	2.7053(16)	2.7503(13)	2.789(2)	2.757(4)
Ca1-C7	2.7713(18)	2.7645(13)	2.843(2)	2.830(4)
Ca1-C8	2.8190(19)	2.8272(14)	2.913(2)	2.978(4)
Ca1-C9	2.8460(18)	2.8710(15)	2.931(2)	3.046(4)
Ca1-C10	2.8581(17)	2.9223(15)	2.913(2)	3.009(4)
Ca1-C11	2.8108(16)	2.8987(14)	2.878(2)	2.873(4)
Average Ca-C_{Aryl}	2.8018	2.839	2.878	2.916
Ca-plane (arene^{DIPP})	2.4199(9)	2.4619(6)	2.5079(11)	2.5391(19)
Ca-centroid (arene^{DIPP})	2.4242(9)	2.4685(6)	2.5121(11)	2.5581(18)

[a] Numbering scheme adopted to those of **2** and **3**. [b] see reference [13] [c] see reference [16].

Complex $^{t\text{Bu}}\text{Am}^{\text{DIPP}}\text{CaN}(\text{SiMe}_3)_2$ (**3**) shows similar behavior. The flexible coordination mode of the $^{t\text{Bu}}\text{Am}^{\text{DIPP}}$ ligand in **3** is nicely illustrated by its synthesis from the corresponding diethyl ether adduct $^{t\text{Bu}}\text{Am}^{\text{DIPP}}\text{CaN}(\text{SiMe}_3)_2(\text{Et}_2\text{O})$. The remarkably facile removal of ether *in vacuo* is accompanied by a change of the coordination mode from *N,N* to *N,Aryl*, as confirmed by XRD (see Figure 2). Structural features of **3** are similar to [$^{t\text{Bu}}\text{Am}^{\text{DIPP}}\text{Ca}]_2$(SD), but the Ca···Aryl contact is somewhat longer (see Table 1). Exchange of the two inequivalent DIPP groups in solution has a significantly smaller activation barrier of $\Delta G^{\ddagger}$ = 14.3 kcal/mol (determined by NMR spectroscopy, see ESI) than observed for **2**, **4** and [$^{t\text{Bu}}\text{Am}^{\text{DIPP}}\text{Ca}]_2$(SD).

The differences in coordination modes have been evaluated by DFT calculations (ωB97XD/def2tzvpp). Calculations on the cationic complex [$^{t\text{Bu}}\text{Am}^{\text{DIPP}}\text{Ca}(\text{C}_6\text{H}_6)]^+$ show that the *N,Aryl* coordination mode is favored over *N,N*-coordination by ΔH = 13.0 kcal/mol. In agreement with experiment a somewhat lower energy difference is found for $^{t\text{Bu}}\text{Am}^{\text{DIPP}}\text{CaN}(\text{SiMe}_3)_2$ (**3**): ΔH = 10.3 kcal/mol. By comparison of the crystal structures of **I**, **1**-**4** and $^{t\text{Bu}}\text{Am}^{\text{DIPP}}\text{CaN}(\text{SiMe}_3)_2(\text{Et}_2\text{O})$, it is clear that the less favorable *N,N*-coordination can only exist when coordinating solvents like Et_2O or THF are present. In these cases, the switch from *N,Aryl*- to *N,N*-coordination creates free coordination sites and the energy needed for this process is compensated for by additional Ca···ether interaction.

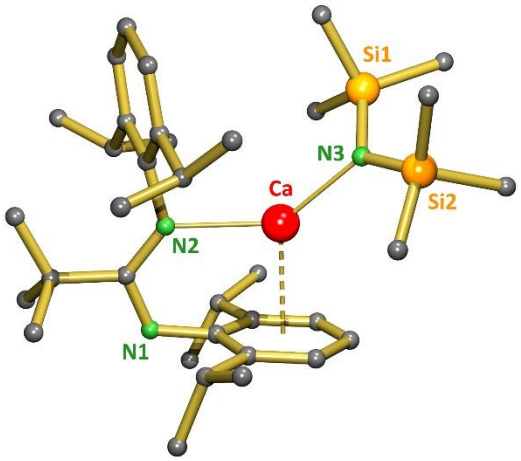

Figure 2. Molecular structure of [$^{t\text{Bu}}\text{Am}^{\text{DIPP}}\text{CaN}(\text{SiMe}_3)_2$]. Hydrogen atoms have been removed for clarity.

Catalyst screening in hydroboration

With the four precatalysts **1**-**4** at hand, their performance in the hydroboration of various ketones using HBpin (4,4,5,5-tetramethyl-1,3,2-dioxaborolane) was investigated (see Table 2). From these observations the following conclusions can be drawn.

Table 2. Hydroborations of ketones $(R^1)(R^2)C=O$ with HBpin at 25°C in benzene/chlorobenzene (1:1).

Entry	R^1	R^2	Catalyst[a,b]	Loading [mol%]	t [min] [c]	Conv. [%][d]
1	Ph	Me	$^{Ph}Am^{iPr}CaI$	3	300	95%
2			**1**	0.5	140	95%
3			**2**	0.5	40	97
4			**3**	0.5	20	>99
5			**4**	0.5	20	>99
6	4-(NO_2)-C_6H_4	Me	$^{Ph}Am^{iPr}CaI$	3	300	73%
7			**1**	0.5	40	>99
8			**2**	0.5	30	>99
9			**3**	0.5	20	>99
10			**4**	0.5	20	>99
11	4-(MeO)-C_6H_4	Me	$^{Ph}Am^{iPr}CaI$	3	300	78%
12			**1**	0.5	130	96
13			**2**	0.5	90	95
14			**3**	0.5	<10	>99
15	*t*Bu	Me	**1**	0.5	40	90%
16			**2**	0.5	20	94%
17			**3**	0.5	<10	>99
18			**4**	0.5	<10	>99
19	Ph	Ph	**2**	5	180	>99
20			**2**	1	180	95
21			**3**	1	<10	>99
22	4-Br-C_6H_4	Me	**2**	1	30	>99
23			**3**	1	<10	>99
24	4-(CF_3)-C_6H_4	Me	**2**	0.5	70	95
25			**3**	0.5	<10	>99
26			**2**	0.05	<10	>99
27			**3**	0.05	<10	>99

[a] Catalysts: $^{tBu}Am^{DIPP}CaX$; X = I^- (**1**), $[B(C_6F_5)_4]^-$ (**2**), $[N(SiMe_3)_2]^-$ (**3**), H^- (**4**). [b] For catalyst $^{Ph}Am^{iPr}CaI$ (**I**) values are taken from reference [12]. [c] Monitored by ^1H NMR in 10 min intervals. [d] Determined by ^1H NMR measurements.

(i) Complex $[^{tBu}Am^{DIPP}CaI(THF)_2]_2$ (**1**), which exists as a iodo-bridged dimer in the solid state, already shows superior performance in comparison to $^{Ph}Am^{iPr}CaI(THF)_3$, used by *Sen* and co-workers (compare entries 1-2, 6-7 and 11-12, Table 2). Since the additional THF ligands in **1** have no influence on the catalysis, because they are rapidly replaced by the ketone substrates and HBpin, which are present in large excess, the difference in reactivity can be solely attributed to the different amidinate spectator ligand. This could be due to difference in ligand bulk between $^{tBu}Am^{DIPP}$ (V_B = 34.0%) and $^{Ph}Am^{iPr}$ (V_B = 28.1%); both in *N,N*-coordination mode. Another difference is the fact that aryl-substituted N's in $^{tBu}Am^{DIPP}$ are much less electron-donating than the alkyl-substituted N's in $^{Ph}Am^{iPr}$ thus making the metal center in $[^{tBu}Am^{DIPP}CaI(THF)_2]_2$ (**1**) more electrophilic.

(ii) In case high electrophilicity of the Ca center is needed for activity, the exchange of the iodide anion for $[B(C_6F_5)_4]^-$ should further increase the performance of the system. Indeed, the activity of the cationic Ca complex **2** is for all substrates consistently higher than that of **1**. Ketones with electron donating or withdrawing groups were rapidly consumed (>94% conversion) in presence of catalyst **2** and the desired hydroboration products formed even with very low catalyst loadings

down to 0.05 mol% (see Table 2). Similar to the calcium amidinate complex $^{Ph}Am^{iPr}CaI(THF)_3$ by Sen and coworkers,[12] the system showed a reasonable functional group tolerance. The high TOF's found for this system (see Table S3 and S4, ESI) are likely related to the increased Lewis acidity of the calcium center in the intermediate $[^{tBu}Am^{DIPP}Ca(substrate)_n]^+[B(C_6F_5)_4]^-$ in comparison to $^{tBu}Am^{DIPP}CaI(substrate)_n$ (substrate = aldehyde, ketone and/or HBpin). Although the coordination mode of the amidinate differs in the precatalysts $[^{tBu}Am^{DIPP}Ca(C_6H_6)]^+[B(C_6F_5)_4]^-$ (**2**: *N,Aryl*) and $[^{tBu}Am^{DIPP}CaI(thf)_2]_2$ (**1**: *N,N*), a significant influence of the *N,Aryl*-coordination mode on catalysis is unlikely. It could be shown that addition of benzaldehyde (as a model substrate) led to a replacement of benzene in **2** and subsequently to a change of the initial *N,Aryl*-coordination mode to a symmetrical *N,N*-coordination, when an excess of substrate is present, as it is during catalysis (see Figure S12, ESI).

(iii) The performance in catalysis of $^{tBu}Am^{DIPP}CaN(SiMe_3)_2$ (**3**) is again clearly higher than that of highly Lewis acidic **2** and an activity similar to that of previously investigated magnesium catalysts was found. For instance, the TOF of 600 h^{-1} in case of benzophenone, which often serves as benchmark substrate, is in the same order of magnitude as Hill's $^{Me}BDI^{DIPP}MgBu$ (500 h^{-1}),[24] Okuda's $[Mg(THF)_6]^{2+}[HBPh_3]^-_2$ (1000 h^{-1})[25] or the phosphinoamido stabilized magnesium hydride used by Stasch (1760 h^{-1} per magnesium center).[26] The much lower TOF's of 8.6 h^{-1} for $^{Ph}Am^{iPr}CaI(THF)_3$ and 32 h^{-1} for $[^{tBu}Am^{DIPP}Ca(C_6H_6)]^+[B(C_6F_5)_4]^-$ (**2**) suggest that these catalysts operate via a different mechanism.

(iv) Our earlier reported Ca hydride complex $[^{tBu}Am^{DIPP}CaH]_2$ (**4**) showed activities which are very similar to those of $^{tBu}Am^{DIPP}CaN(SiMe_3)_2$ (**3**). It is therefore likely that catalysts **3** and **4** operate through a metal hydride mechanism that is generally accepted for Mg catalysts of type LMgR (L = spectator ligand and R = active group).[3,24,26]

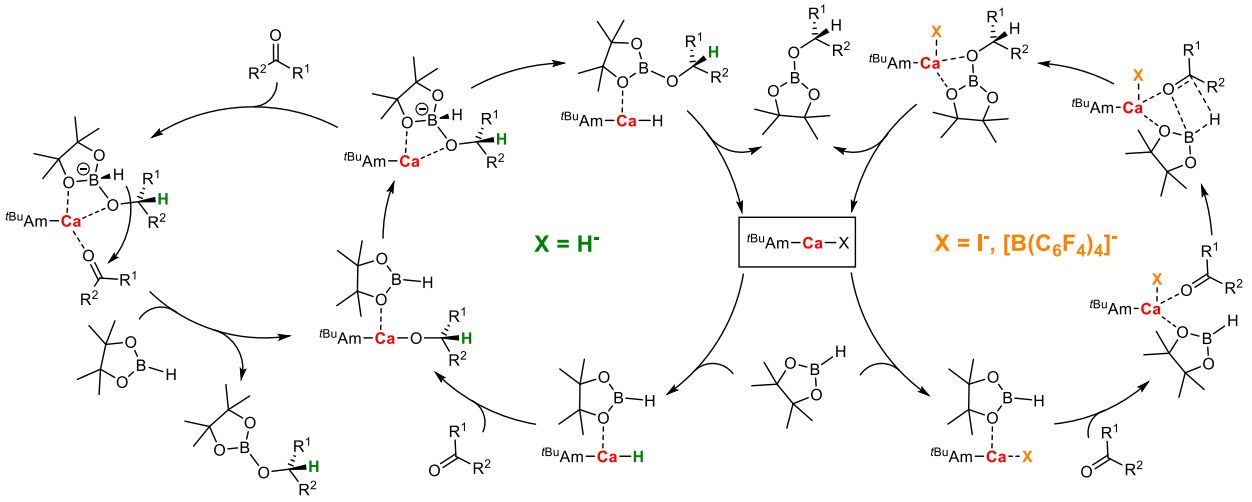

Scheme 3. Proposed catalytic cycles for the hydroboration of ketones by calcium catalysts containing different ligands. For X = $(Me_3Si)_2N^-$ we assume prior hydride formation and the hydride mechanism.

The intermediacy of a hydride complex is obvious in case of **4** or Stasch's Mg hydride catalyst, where the hydride is already present, or in case of $[^{Me}BDI^{DIPP}MgBu]$, where the formation of $[^{Me}BDI^{DIPP}MgH]_2$ upon reaction with HBpin was conclusively proven.[24] In case of Okuda's $[Mg(thf)_6][HBPh_3]_2$ catalyst, transfer of a hydride from the boron center of the anion to magnesium (or directly to the substrate) seems feasible.[25] In $[Mg(THF)_6][HB(C_6F_5)_3]_2$, however, such transfer is impeded by the higher Lewis acidity of the boron center, which is likely the reason for the inferior catalytic activity of this system.[25] Calcium complexes containing a $(Me_3Si)_2N^-$ group are also known as excellent precursors for the formation of calcium hydride complexes, *e.g.* by reaction with $PhSiH_3$, and it may be envisioned that the well-known complex $[^{tBu}Am^{DIPP}CaH]_2$ forms under catalytic conditions as well.

Alternative to a hydride cycle is a pathway in which the hydride is not transferred from the metal to the ketone but directly from the borate (Scheme 3, far left). Indications that hydroboration not necessarily proceeds through the intermediacy of a metal hydride complex come from our group's previous studies of pyridine hydroboration.[27] This conclusion was based on differences in regioselectivity between stoichiometric metal hydride reactions and catalytic conversions.

Catalysts **I**, **1** and **2** do not contain active groups and it is *a priori* not clear how in this case intermediate hydride or borate species could be formed. Since the activity for this groups of catalysts increases with increasing Lewis acidity, we propose a mechanism in which the metal's Lewis acidity plays a central role. It could be envisioned that HBpin and the ketone both bind to the Ca^{2+} metal center. Polarization of the C=O bond subsequently leads to hydride transfer and concomitant B-O bond

formation. This direct B-H/C=O addition mechanism is similar to that proposed for catalyst-free ketone hydroboration.[28] Ketone hydroboration by Lewis acidic Ca complexes could best be interpreted by considering the Ca^{2+} metal as a connector that brings both substrates in close vicinity. This compensates for the considerable entropy loss in ketone hydroboration.
Hydroboration of aldehydes was also briefly tested, but due the ease of this transformation and the resulting higher reaction rates, differences between the different catalysts are less pronounced (compare ESI, Table S3).

Conclusion

We have prepared a series of Ca amidinate complexes with the amidinate ligand $^{t\text{Bu}}Am^{DIPP}$. This bulky ligand is able to saturate the coordination sphere of large metal ions like Ca^{2+} by *N,Aryl*- or *N,N*-chelation. *N,N*-coordination is typically observed when coordinating solvents are present, *e.g.* in $[^{t\text{Bu}}Am^{DIPP}CaI(THF)_2]_2$ (**1**) or $^{t\text{Bu}}Am^{DIPP}CaN(SiMe_3)_2(Et_2O)$, or when there is not enough space available for *N,Aryl*-coordination, *e.g.* in homoleptic $(^{t\text{Bu}}Am^{DIPP})_2Ca$. The buried volume for the ligand with *N,Aryl*-coordination is comparable to that of the widely known ß-diketiminate ligand $^{Me}BDI^{DIPP}$. Using $^{t\text{Bu}}Am^{DIPP}$ we achieved the isolation of the first "naked" (Lewis base-free) cationic Ca amidinate complex $[^{t\text{Bu}}Am^{DIPP}Ca(C_6H_6)]^+[B(C_6F_5)_4]^-$ (**2**) in which the ligand is bound by *N,Aryl*-chelation. This coordination mode was also found in ether-free $^{t\text{Bu}}Am^{DIPP}CaN(SiMe_3)_2$ (**3**). In solution, the fast exchange between *N,Aryl*- and *N,N*-coordination modes is more facile in $^{t\text{Bu}}Am^{DIPP}CaN(SiMe_3)_2$ ($\Delta G^{\ddagger}$ = 14.3 kcal/mol) than in the cation $[^{t\text{Bu}}Am^{DIPP}Ca(C_6H_6)]^+$ ($\Delta G^{\ddagger}$ = 16.1 kcal/mol). This likely originates from the higher Lewis acidity of the metal in the cationic complex.
We demonstrated that calcium complexes bearing the highly flexible amidinate ligand $^{t\text{Bu}}Am^{DIPP}$ are suitable catalysts for the hydroboration of ketones and aldehydes. Since catalysts **1**-**4** carry the same spectator ligand the influence of the second anionic ligand or counter anion could be evaluated. The anion or counter ion X^- in the catalysts $^{t\text{Bu}}Am^{DIPP}CaX$ significantly influences the performance of the system and activities increase along the series $I^- < B(C_6F_5)_4^- < (Me_3Si)_2N^- \approx H^-$. For the first two catalysts with I^- or $B(C_6F_5)_4^-$, catalyst activities increase with the Lewis acidity of the metal. However, compared to these catalysts, Ca complexes with $X^- = (Me_3Si)_2N^-$ or H^- are by far superior. They could be considered being competitive with previously reported magnesium based catalysts.
We propose two independently operating mechanisms. For $^{t\text{Bu}}Am^{DIPP}CaX$ complexes with an unreactive ligand X^-, like I^- or $[B(C_6F_5)_4]^-$, a Lewis acid mechanism is likely while catalysts with a reactive ligand X^-, like $(Me_3Si)_2N^-$ or H^- must operate through a mechanism which involves intermediate metal hydride (or borate) complexes.

Experimental

All experiments were conducted under an inert nitrogen atmosphere using standard Schlenk and glovebox techniques (MBraun, Labmaster SP). Benzene, toluene and hexane were degassed with nitrogen, dried over activated aluminium oxide (Solvent Purification System: Pure Solv 400-4-MD, Innovative Technology) and stored over 3 Å molecular sieves unless otherwise noted. Chlorobenzene was dried over calcium hydride, distilled under N_2 atmosphere and stored over molecular sieves 3Å. C_6D_6, C_6D_5Br and $CDCl_3$ were dried over 3Å molecular sieves. $[Ph_3C]^+[B(C_6F_5)_4]^-$ (Boulder Scientific), 4'-nitroacetophenone, 4-chlorobenzaldehyde, 4-cyanobenzaldehyde, HBpin, 4'-bromocetophenone, mesitylaldehyde, benzophenone, 4`-methoxyacetophenone and 4'-(trifluoromethyl)acetophenone were used as received. Benzaldehyde, cyclohexanone, pinacolone and acetophenone were dried over molecular sieves 3Å, distilled and stored under N_2 atmosphere. $^{t\text{Bu}}Am^{DIPP}H$,[15] $^{t\text{Bu}}Am^{DIPP}CaN(SiMe_3)_2(Et_2O)$,[14] $[^{t\text{Bu}}Am^{DIPP}CaI(THF)_2]_2$,[13] $[^{t\text{Bu}}Am^{DIPP}CaH]_2$[14] and $[H(OEt_2)_2]^+[B(C_6F_5)_4]^-$[29] were synthesized according to literature procedures. NMR spectra were recorded with a Bruker Avance III HD 400 MHz or a Bruker Avance III HD 600 MHz spectrometer. The spectra were referenced to the respective residual signals of the deuterated solvents. Elemental analysis was performed with a Euro EA 3000 (Euro Vector) analyzer. All crystal structures have been measured on a SuperNova (Agilent) diffractometer with dual Cu and Mo microfocus sources and an Atlas S2 detector.

Synthesis of $[^{t\text{Bu}}Am^{DIPP}H_2]^+[B(C_6F_5)_4]^-$. A mixture of $[H(OEt_2)_2]^+[B(C_6F_5)_4]^-$ (254.7 mg, 0.3075 mmol) and $^{t\text{Bu}}Am^{DIPP}H$ (142.4 mg, 0.3385 mmol) was dissolved in 3 mL of chlorobenzene and the resulting colorless solution was stirred overnight at ambient temperature. All volatiles were removed *in vacuo*. The resulting white solid was triturated two times with 2 mL of hexane. Drying *in vacuo* afforded $[^{t\text{Bu}}Am^{DIPP}H_2]^+[B(C_6F_5)_4]^-$ as a fine white powder in almost quantitative yield: 316.8 mg, 94%. ^{1}H NMR (400 MHz, C_6D_5Br, 298K): δ/ppm 0.75 (d, $^3J_{HH}$ = 7 Hz, 6H, CH*Me*$_2$), 1.06-1.00 (m, 15H, C*Me*$_3$, CH*Me*$_2$), 1.13 (d, $^3J_{HH}$ = 7 Hz, 6H, CH*Me*$_2$), 1.23 (d, $^3J_{HH}$ = 7 Hz, 6H, CH*Me*$_2$), 2.63 (hept, $^3J_{HH}$ = 7 Hz, 2H, C*H*Me$_2$), 2.71 (hept, $^3J_{HH}$ = 7 Hz, 2H, C*H*Me$_2$), 6.93 (d, $^3J_{HH}$ = 8 Hz, 2H, Ar*H*), 7.16 (d, $^3J_{HH}$ = 8 Hz, 2H, Ar*H*), 7.21 (t, $^3J_{HH}$ = 8 Hz, 1H, Ar*H*), 7.36-7.28 (m, 2H, N*H*, Ar*H*, partly omitted by solvent signal), 7.50 (s, 1H, N*H*). ^{13}C{^{1}H} NMR (101 MHz, C_6D_5Br, 298K): δ/ppm 21.42 (CH*Me*$_2$), 22.00 (CH*Me*$_2$),

25.28 (CH*Me*$_2$), 25.37 (CH*Me*$_2$), 28.40 (C*Me*$_3$), 29.44 (2x C*H*Me$_2$), 29.62 (2x C*H*Me$_2$), 39.26 (*C*Me$_3$), 125.09 (2x *C*H-Ar), 126.05 (2x *C*H-Ar), 128.80 (N*C*-Ar), 128.80 (N*C*-Ar), 132.05 (*C*H-Ar), 133.52 (*C*H-Ar), 145.34 (2x *C*-Ar), 146.22 (2x *C*-Ar), 175.09 (*C*(CMe$_3$)=NAr). [BAr^F]$^-$ was not observed. ^{19}F{^{1}H} NMR (376 MHz, C_6D_5Br, 298K): δ/ppm -131.5z (s), -162.1 (t , $^3J_{FF}$ = 21 Hz, Ar*F*), -166.0 (m). ^{11}B{^{1}H} NMR (128 MHz, C_6D_5Br, 298K): δ/ppm -16.1 (s). Anal. Calcd. for $C_{53}H_{45}BF_{20}N_2$ (MW: 1100.74 g/mol): C, 57.83; H, 4.12; N, 2.55. Found: C, 57.84; H, 4.16; N, 2.47.

Synthesis of ^{tBu}Am^{DIPP}CaN(SiMe$_3$)$_2$ (3). 413.0 mg of $^{t\text{Bu}}$Am$^{\text{DIPP}}$CaN(SiMe$_3$)$_2$(Et$_2$O) (0.5949 mmol) were dissolved in 15 ml of toluene. All volatiles were then removed *in vacuo*. This procedure was repeated two times. The resulting off-white solid was dissolved in 1.5 mL of hexane. Crystals could be obtained by storing the solution at -30°C overnight. The crystals were dried *in vacuo* to a yield $^{t\text{Bu}}$Am$^{\text{DIPP}}$CaN(SiMe$_3$)$_2$ as white solid. Yield: 293.7 mg, 80%.

^{1}H NMR (400 MHz, toluene-d$_8$, 243K): δ/ppm -0.00 (s, 18H, N(Si*Me*$_3$)$_2$), 1.18 (d, $^3J_{HH}$ = 6.8 Hz, 6H, CH*Me*$_2$), 1.22 (d, $^3J_{HH}$ = 6.7 Hz, 6H, CH*Me*$_2$), 1.28 (d, $^3J_{HH}$ = 6.5 Hz, 6H, CH*Me*$_2$), 1.31 (d, $^3J_{HH}$ = 6.5 Hz, 6H, CH*Me*$_2$), 1.50 (s, 9H, C*Me*$_3$), 2.96 (hept, $^3J_{HH}$ = 6.8 Hz, 2H, C*H*Me$_2$), 3.37 (hept, $^3J_{HH}$ = 6.8 Hz, 2H, C*H*Me$_2$), 6.87-6.98 (m, 6H, 6x Ar*H*). ^{13}C{^{1}H} NMR (101 MHz, toluene-d8, 243K): δ/ppm 5.70, 5.75 (Si*Me*$_3$), 21.03 (2x *C*HMe$_2$), 23.64 (CH*Me*$_2$), 24.24 (CH*Me*$_2$), 25.52 (CH*Me*$_2$), 28.79 (2x *C*HMe$_2$), 28.87 (CH*Me*$_2$), 31.55 (C*Me*$_3$), 42.31 (*C*Me$_3$), 121.16 (*C*H-Ar), 123.01 (*C*H-Ar), 124.62 (2x *C*H-Ar), 124.92 (2x *C*H-Ar), 139.73 (2x *C*-Ar), 144.67 (2x *C*-Ar), 145.65 (N*C*-Ar), 160.19 (N*C*-Ar), 170.23 (*C*(CMe$_3$)=NAr). Anal. Calcd. for $C_{35}H_{61}BCaN_3Si_2$ (MW: 620.14 g/mol): C, 67.79; H, 9.92; N, 6.78. Found: C, 68.02; H, 10.07; N, 6.57.

Synthesis of [^{tBu}Am^{DIPP}Ca(C$_6$H$_6$)]$^+$[B(C$_6$F$_5$)$_4$]$^-$. A solution of 480.9 mg (0.5214 mmol) [Ph$_3$C]$^+$[B(C$_6$F$_5$)$_4$]$^-$ in 2 mL of chlorobenzene was added slowly to a suspension of 240.3 mg (0.2608 mmol) [$^{t\text{Bu}}$Am$^{\text{DIPP}}$CaH]$_2$ in 2 mL of chlorobenzene. The resulting yellow suspension was stirred overnight and all volatiles were removed *in vacuo*. Addition of benzene (2 mL) to the yellow foam led to the formation of two phases. The upper phase was removed and the lower phase was washed with benzene (5x2 mL). Crystals could be obtained by storing the biphasic system at room temperature over several days. Crystallization can be forced by addition of seeding crystals. The obtained crystals have to be further purified by thermal diffusion in an 1:4 mixture of benzene:hexane at 65 °C (see ESI, Figure S11). Yield: 392.4 mg (62%).

^{1}H NMR (600 MHz, C_6D_5Br, 298K): δ/ppm 0.82 (d, $^3J_{HH}$ = 6.6 Hz, 6H, CH*Me*$_2$), 1.27-1.16 (m, 27H, C*Me*$_3$, 3x CH*Me*$_2$), 3.03 (hept, $^3J_{HH}$ = 6.3 Hz, 2H, C*H*Me$_2$), 3.21 (hept, $^3J_{HH}$ = 6.3 Hz, 2H, C*H*Me$_2$), 6.84 (d, $^3J_{HH}$ = 7.6 Hz, 2H, Ar*H*), 6.91 (t, $^3J_{HH}$ = 7.6 Hz, 1H, Ar*H*), 7.11 (t, $^3J_{HH}$ = 7.5 Hz, 1H, Ar*H*), 7.01 (partly omitted by solvent, 2H, Ar*H*), 7.21 (s, 6H, benzene). ^{13}C{^{1}H} NMR (101 MHz, C_6D_5Br, 298K): δ/ppm 20.5 (CH*Me*$_2$), 22.6 (CH*Me*$_2$), 23.4 (CH*Me*$_2$), 28.2 (2x *C*HMe$_2$), 28.3 (CH*Me*$_2$), 29.3 (2x *C*HMe$_2$), 31.3 (C*Me*$_3$), 41.7 (*C*Me$_3$), 121.4 (*C*H-Ar), 124.3 (2x *C*H-Ar), 125.7 (2x *C*H-Ar), 125.9 (*C*H-Ar), 128.6 (benzene), 137.0 (d, $^1J_{CF}$ = 238 Hz, [B(C$_6$F$_5$)$_4$]), 138.5 (d, $^1J_{CF}$ = 249 Hz, [B(C$_6$F$_5$)$_4$]), 142.3 (2x *C*-Ar), 142.5 (N*C*-Ar), 147.0 (2x *C*-Ar), 148.7 (d, $^1J_{CF}$ = 232 Hz, [B(C$_6$F$_5$)$_4$]$^-$), 162.4 (N*C*-Ar), 171.8 (*C*(CMe$_3$)=NAr). ^{19}F{^{1}H} NMR (565 MHz, C_6D_5Br, 298K): δ/ppm -131.7 (s), -159.2 (t, $^3J_{FF}$ = 21 Hz, Ar*F*), -164.1 (m). ^{11}B{^{1}H} NMR (193 MHz, C_6D_5Br, 298K): δ/ppm -16.39 (s). Anal. Calcd. for $C_{59}H_{49}BCaF_{20}N_2$ (MW: 1216.91 g/mol): C, 58.23; H, 4.06; N, 2.30. Found: C, 59.30; H, 4.04; N, 2.16.

Catalytic hydroboration of aldehydes and ketones. For catalysts **1**-**3** 0.82 mM and 8.22 mM stock solutions in chlorobenzene were prepared. Since catalyst **4** is insoluble in chlorobenzene, a 8.22 mM stock solution in THF was prepared. For catalytic runs with 0.05-1 mol% catalyst loadings, the following quantities of stock solutions have been used: 0.05 mol% (60 µL, 0.82 mM), 0.5 mol% (60 µL, 8.22 mM), 1 mol% (120 µL, 8.22 mM). Catalytic experiments with catalysts **1**-**3** have been performed in a 2/1 chlorobenzene/C_6D_6 solution (400 µL chlorobenzene, 200 µL C_6D_6). Catalytic experiments with **4** were run in a THF/chlorobenzene/C_6D_6 mixture (60 µL THF, 340 µL chlorobenzene, 200 µL C_6D_6). This means that the given amount of stock solutions was filled up with chlorobenzene to a total volume of 400 µL and subsequently an additional 200 µL of C_6D_6 was added (the latter was used for D-locking during ^{1}H NMR monitoring). For the higher catalyst loading of 5 mol% the catalyst was weighed in as a pure substance and dissolved in 400 µL of chlorobenzene and 200 µL of C_6D_6. After addition of 14.3 µL HBpin (98.6 µM), the sample was thoroughly mixed and the first ^{1}H NMR spectrum was recorded within 10 min. The reaction was monitored by ^{1}H NMR in 10 min intervals. Upon completion of the reaction, the solvent was removed *in vacuo* and $CDCl_3$ was added. NMR data and spectra can be found in the supporting information.

Crystal structure determinations. Using Olex2,[30] the structure was solved by Intrinsic Phasing (ShelXT)[31] and refined with ShelXL[32] using Least Squares minimization. All non-hydrogen atoms were refined with anisotropic displacement parameters. All hydrogen atoms were placed in ideal positions and refined as riding atoms with relative isotropic displacement parameters. Crystal data and experimental methods can be found in the Supporting Information. The crystal structure data has been deposited with the Cambridge Crystallographic Data Centre. CCDC 1990324 contains the supplementary crystallographic data for complex [$^{t\text{Bu}}$Am$^{\text{DIPP}}$Ca(C$_6$H$_6$)]$^+$[B(C$_6$F$_5$)$_4$]$^-$·C$_6$H$_6$ (**2**). CCDC 1990325 contains the supplementary crystallographic data for complex $^{t\text{Bu}}$Am$^{\text{DIPP}}$CaN(SiMe$_3$)$_2$ (**3**). CCDC 1990326 contains the supplementary crystallographic data for complex [$^{t\text{Bu}}$Am$^{\text{DIPP}}$H$_2$]$^+$[B(C$_6$F$_5$)$_4$]$^-$. CCDC 1990327 contains the supplementary crystallographic data for complex ($^{t\text{Bu}}$Am$^{\text{DIPP}}$)$_2$Ca. This data can be obtained free of charge from The Cambridge Crystallographic Data Centre via www.ccdc.cam.ac.uk/data_request/cif.

References

[1] *Early Main Group Metal Catalysis – Concepts and Reactions*, Ed. S. Harder, Wiley-VCH, **2020**, Weinheim, Germany.

[2] S. Harder, *Chem. Rev.* **2010**, 110, 3852–3876.

[3] M. S. Hill, D. J. Liptrot, C. Weetman, *Chem. Soc. Rev*. **2016**, *45*, 972–988.

[4] L. C. Wilkins, R. L. Melen, *Coord. Chem. Rev*. **2016**, *324*, 123–139.

[5] a) S. Harder, *Angew. Chem., Int. Ed.* **2004**, *43*, 2714–2718. b) N. Ajellal, J.-F. Carpentier, C. Guillaume, S. M. Guillaume, M. Helou, V. Poirier, Y. Sarazin, A. Trifonov, *Dalton Trans.* **2010**, *39*, 8363-8376. c) I. Yildirim, S. Crotty, C. H. Loh, G. Festag, C. Weber, P.-F. Caponi, M. Gottschaldt, M. Westerhausen, U. S. Schubert, *J. Polym. Sci. Part A Polym. Chem.* **2016**, *54*, 437–448.d) I. Yildirim, T. Yildirim, D. Kalden, G. Festag, N. Fritz, C. Weber, S. Schubert, M. Westerhausen, U. S. Schubert, *Polym. Chem.* **2017**, *8*, 4378–4387.

[6] a) S. Harder, J. Martin, C. Knüpfer, J. Eyselein, C. Färber, S. Grams, J. Langer, K. Thum, M. Wiesinger, *Angew. Chem., Int. Ed.* **2020**, DOI 10.1002/anie.202001160. b) H. Bauer, M. Alonso, C. Färber, H. Elsen, J. Pahl, A. Causero, G. Ballmann, F. De Proft, S. Harder, *Nat. Catal.* **2018**, *1*, 40–47. c) H. Bauer, K. Thum, M. Alonso, C. Fischer, S. Harder, *Angew. Chem., Int. Ed.* **2019**, *58*, 4248–4253. d) D. Schuhknecht, C. Lhotzky, T. P. Spaniol, L. Maron, J. Okuda, *Angew. Chem., Int. Ed.* **2017**, *56*, 12367–12371. e) A. S. S. Wilson, C. Dinoi, M. S. Hill, M. F. Mahon, L. Maron, *Angew. Chem., Int. Ed.* **2018**, *57*, 15500–15504. f) X. Shi, G. Qin, Y. Wang, L. Zhao, Z. Liu, J. Cheng, *Angew. Chem., Int. Ed.* **2019**, *58*, 4356–4360.

[7] a) J. Intemann, H. Bauer, J. Pahl, L. Maron, S. Harder, *Chem. - Eur. J.* **2015**, *21*, 11452–11461. b) H. Elsen, C. Fischer, C. Knüpfer, A. Escalona, S. Harder, *Chem. - Eur. J.* **2019**, *25*, 16141–16147. c) D. Schuhknecht, T. P. Spaniol, L. Maron, J. Okuda, *Angew. Chem., Int. Ed.* **2020**, *59*, 310–314. d) D. Mukherjee, D. Schuhknecht, J. Okuda, *Angew. Chem., Int. Ed.* **2018**, *57*, 9590–9602. e) L. Garcia, M. F. Mahon, M. S. Hill, *Organometallics* **2019**, *38*, 3778–3785. f) P. Jochmann, J. P. Davin, T. P. Spaniol, L. Maron, J. Okuda, *Angew. Chem., Int. Ed.* **2012**, *51*, 4452–4455.

[8] a) M. R. Crimmin, M. Arrowsmith, A. G. M. Barrett, I. J. Casely, M. S. Hill, P. A. Procopiou, *J. Am. Chem. Soc.* **2009**, *131*, 9670–9685. b) M. R. Crimmin, I. J. Casely, M. S. Hill, *J. Am. Chem. Soc.* **2005**, *127*, 2042–2043. c) S. Krieck, D. Kalden, A. Oberheide, L. Seyfarth, H.-D. Arndt, H. Görls, M. Westerhausen, *Dalton Trans.* **2019**, *48*, 2479–2490. d) S. Ziemann, S. Krieck, H. Görls, M. Westerhausen, *Organometallics* **2018**, *37*, 924–933. e) N. Romero, S.-C. Roşca, Y. Sarazin, J.-F. Carpentier, L. Vendier, S. Mallet-Ladeira, C. Dinoi, M. Etienne, *Chem. - Eur. J.* **2015**, *21*, 4115–4125. f) J. Penafiel, L. Maron, S. Harder, *Angew. Chem., Int. Ed.* **2015**, *54*, 201–206.

[9] a) S.-C. Roşca, T. Roisnel, V. Dorcet, J.-F. Carpentier, Y. Sarazin, *Organometallics* **2014**, *33*, 5630–5642. b) J. Pahl, T. E. Stennett, M. Volland, D. M. Guldi, S. Harder, *Chem. - Eur. J.* **2019**, *25*, 2025–2034. c) M. R. Crimmin, A. G. M. Barrett, M. S. Hill, P. B. Hitchcock, P. A. Procopiou, *Organometallics* **2007**, *26*, 2953–2956. d) T. M. A. Al-Shboul, H. Görls, M. Westerhausen, *Inorg. Chem. Commun.* **2008**, *11*, 1419–1421. e) A. O. Tolpygin, A. V. Cherkasov, G. K. Fukin, T. A. Kovylina, K. A. Lyssenko, A. A. Trifonov, *Eur. J. Inorg. Chem.* **2019**, *2019*, 4289–4296. f) I. V. Basalov, B. Liu, T. Roisnel, A. V. Cherkasov, G. K. Fukin, J.-F. Carpentier, Y. Sarazin, A. A. Trifonov, *Organometallics* **2016**, *35*, 3261–3271. g) F. M. Younis, S. Krieck, T. M. A. Al-Shboul, H. Görls, M. Westerhausen, *Inorg. Chem.* **2016**, *55*, 4676–4682.

[10] a) S. Narasimhan, K. G. Prasad, S. Madhavan, *Tetrahedron Lett.* **1995**, *36*, 1141–1144. b) J. Spielmann, S. Harder, *J. Organometal. Chem.* **2012**, *698*, 7-14.

[11] a) T. Suzuki, N. Yamagiwa, Y. Matsuo, S. Sakamoto, K. Yamaguchi, M. Shibasaki, R. Noyori, *Tetrahedron Lett.* **2001**, *42*, 4669–4671. b) T. Tsubugo, Y. Yamashita, S. Kobayashi *Chiral Ca-, Sr-, and Ba-Catalyzed Asymmetric Direct-Type Aldol, Michael, Mannich, and Related Reactions*, Ed. S. Harder, Springer-Verlag, **2013**, Springer, Berlin, Heidelberg, Germany, c) T. Tsubogo, S. Shimizu, S. Kobayashi, *Chem. - Asian J.* **2013**, *8*, 872–876. d) J. M. Begouin, M. Niggemann, *Chem. Eur. J.* **2013**, *19*, 8030-8041.

[12] S. Yadav, S. Pahar, S. S. Sen, *Chem. Commun*. **2017**, *53*, 4562–4564.

[13] A. Causero, H. Elsen, G. Ballmann, A. Escalona, S. Harder, *Chem. Commun*. **2017**, *53*, 10386–10389.

[14] A. Causero, G. Ballmann, J. Pahl, H. Zijlstra, C. Färber, S. Harder, *Organometallics* **2016**, *35*, 3350–3360.

[15] C. Loh, S. Seupel, H. Görls, S. Krieck, M. Westerhausen, *Eur. J. Inorg. Chem*. **2014**, 1312–1321.

[16] A. Causero, H. Elsen, J. Pahl, S. Harder, *Angew. Chem., Int. Ed*. **2017**, *56*, 6906–6910.

[17] S. Yadav, V. S. V. S. N. Swamy, R. Gonnade, S. S. Sen, *ChemistrySelect* **2017**, *1*, 1066–1071.

[18] a) F. T. Edelmann, in *Adv. Organomet. Chem.* Eds.: A. F. Hill, M. J. Fink, Elsevier Inc., **2008**, pp. 183–352. b) T. Chlupatý, A. Růžička, *Coord. Chem. Rev.* **2016**, *314*, 103–113. c) C. Jones, *Coord. Chem. Rev.* **2010**, *254*, 1273–1289. d) P. C. Junk, M. L. Cole, *Chem. Commun.* **2007**, 1579.

[19] L. Garcia, M. D. Anker, M. F. Mahon, L. Maron, M. S. Hill, *Dalton Trans*. **2018**, *47*, 12684–12693.

[20] J. Pahl, S. Brand, H. Elsen, S. Harder, *Chem. Commun*. **2018**, *54*, 8685–8688.

[21] S. Brand, H. Elsen, J. Langer, W. A. Donaubauer, F. Hampel, S. Harder, *Angew. Chem., Int. Ed*. **2018**, *57*, 14169–14173.

[22] J. Pahl, A. Friedrich, H. Elsen, S. Harder, *Organometallics* **2018**, *37*, 2901–2909.
[23] A. Friedrich, J. Pahl, H. Elsen, S. Harder, *Dalton Trans*. **2019**, *48*, 5560–5568.
[24] M. Arrowsmith, T. J. Hadlington, M. S. Hill, G. Kociok-Köhn, *Chem. Commun*. **2012**, *48*, 4567.
[25] D. Mukherjee, S. Shirase, T. P. Spaniol, K. Mashima, J. Okuda, *Chem. Commun*. **2016**, *52*, 13155–13158.
[26] L. Fohlmeister, A. Stasch, *Chem. - Eur. J.* **2016**, *22*, 10235–10246.
[27] J. Intemann, M. Lutz, S. Harder *Organometallics* **2014**, *33*, 5722–5729.
[28] W. Wang, M. Luo, W. Yao, M. Ma, S. A. Pullarkat, L. Xu, P.-H. Leung *New J. Chem.*, **2019**,*43*, 10744-10749.
[29] P. Jutzi, C. Müller, A. Stammler, H. Stammler, *Organometallics* **2000**, *19*, 1442–1444.
[30] O. V. Dolomanov, L. J. Bourhis, R. J. Gildea, J. A. K. Howard, H. Puschmann, *J. Appl. Crystallogr*. **2009**, *42*, 339–341.
[31] G. M. Sheldrick, *Acta Crystallogr. Sect. A Found. Adv*. **2015**, *71*, 3–8.
[32] G. M. Sheldrick, *Acta Crystallogr. Sect. C Struct. Chem*. **2015**, *71*, 3–8.

Acknowledgments

We thank Jochen Schmidt for support with NMR measurements and Antigone Roth for elemental analyses.